CrystEngComm

Accepted Manuscript

ROYAL SOCIETY OF CHEMISTRY

www.rsc.org/crystengcomm

Journal Name

RSCPublishing

ARTICLE

Cite this: DOI: 10.1039/x0xx00000x
Received 00th January 2012,
Accepted 00th January 2012
DOI: 10.1039/x0xx00000x
www.rsc.org/

Toward one-pot manipulating the nickel shape and catalytic performance: from sphere, chain to urchin

Lin Chen, Minling Fang, Chengzhan Liu, Xianchun Liu* and Shuangxi Xing*

Different morphological nickel particles, including spheres, chains and urchins were achieved in ethylene glycol solvent upon simply tuning both the amount of water and NaOH. The synthesis route was based on a routine solvothermal technique, in which nickel chloride and hydrazine hydrate took as nickel source and reductant, respectively. The shape transformation might be induced by an accelerated reaction rate and the change of the polarity of the solvent. Owing to the various morphology, these three kinds of nickel particles presented different catalytic performance. The reduction of 4-nitrophenol by $NaBH_4$ as a typical catalytic model revealed the urchin-like nickel particles behaved the highest catalytic effect because of their unique structure with tips on the surface, which endowed much more active sites for the catalytic reaction. The good magnetic property allowed these nickel particles to be readily recycled after application and they presented much high cycling stability.

Introduction

Shape manipulation has been an interesting issue for a long period of time in nanoscience owing to many shape-depended properties, such as catalysis and electrochemistry performance.[1-4] Typically, the morphology control process in one fixed system could be achieved by tuning the temperature, the amounts of reactants, the type of surfactants, and so on.[5-10] The fine tuning morphology in such a control way makes the materials facile to be utilized in corresponding fields and the best performance can be readily achieved thereby.

Nickel as an important magnetic material has been applied in many fields, including magnetic sensor, catalysis, biomedicine and so on. [11-16]Up to now, kinds of morphological nickel particles, such as spheres, fibers, flower and urchin-like particles have been constructed via different strategies.[17-21]（引用 Mater Res Bull） In these above methods, various reductants, solvents and surfactants were used during hydrothermal, thermal decomposition and microwave-assistance processes. In most cases, the dependence of the nickel morphology on different factors has been investigated based on tuning the concentration of reactants, pH value, the ratio of two solvents and temperature. For example, in a polyol process, changing the ratio of water to 1,2-propanediol could lead to the transformation of urchin to flower-like shapes.[22]

Although many mechanisms have been proposed for the formation of various morphological nickel nanostructures, some deeper studies are required in order to construct appropriate systems for achieving special nanostructures in a facile way. In this report, we provided a simple route to synthesize nickel particles using a solvothermal process in the presence of ethylene glycol as solvent, nickel chloride as nickel source and hydrazine hydrate as reductant. We found a shape transformation from spheres to chains and finally urchin-like nanostructures was realized by co-tuning the amount of water and NaOH. Furthermore, the catalytic performance was evaluated based on the reduction of 4-nitrophenol (4-NP) by $NaBH_4$ as a model reaction. The results illustrated the best catalytic effect of the urchin-like structured nickel particles.

Experiments

Materials

Nickel chloride hexahydrate ($NiCl_2 \cdot 6H_2O$), hydrazine hydrate ($N_2H_4 \cdot H_2O$; 80 wt%) were purchased from Tianjin Chemical Reagent Co., Ltd. Ethylene glycol (EG) and sodium hydroxide were obtained from Beijing Chemical Reagent Co., Ltd. 4-NP was purchased from Shanghai Chemical Reagent Co., Ltd. Sodium borohydride was obtained from Sinopharm Chemical Reagent Co., Ltd. All the chemicals were used without further purification.

Synthesis of nickel particles

In a typical synthesis，0.0685 g of $NiCl_2 \cdot 6H_2O$ was dissolved in 30 mL of EG. After that, a certain volume of NaOH aqueous solution (1 M) was added into the above solution under continuous stirring followed by the addition of $N_2H_4 \cdot H_2O$ (500 μL). The mixture was transferred into a 50 mL Teflon-lined autoclave. The autoclave was sealed and maintained at 110 °C for 4 h. After the autoclave was cooled down to room temperature, the resulting black precipitates were collected by a magnet and washed several times with distilled water and absolute ethanol. Finally, the products were dried in a vacuum at 60 °C for 8 h. The pH of the reaction system before the addition of NaOH was 9.40; while it increased to 11.30 and 12.30 after adding 0.5 and 2 mL of NaOH, respectively.

Characterization

The morphology of the products was characterized by transmission electron microscope (TEM, Hitachi-H7700) and scanning electron microscopy (SEM, JEOL SM-6360LV). The X-ray diffraction (XRD) measurements were taken on a Siemens D5005 Diffractometer with Cu Kα radiation (λ = 1.5418Å). The UV–vis spectra of the products were detected with a UV–vis spectrometer (UV-2550). The magnetization measurements of the products were performed on a superconducting quantum interference device (SQUID) magnetometer (Quantum Design). The M–H measurements were performed with an applied field range of ±10000 Oe at 300 K. The gas adsorption-desorption experiments were performed on automatic volumetric adsorption equipment (V-Sorb 2800S).

Catalytic reaction of 4-NP

For the catalysis experiments, 100 μL of the as-prepared catalysts in aqueous dispersion (0.5 mg mL^{-1}) were mixed with 2 mL of 4-NP aqueous solution (0.12 mM). Next, 1 mL of fresh $NaBH_4$ solution (100 mM) was added to the above mixture. The quantity of the catalyst in the system is 0.05 mg. The UV-Vis spectra of the solution were recorded at every 1 min interval.

Results and Discussion

TEM and SEM

The TEM images of the nickel particles obtained from three synthetic systems containing 0, 0.5 and 2 mL of NaOH aqueous solutions are shown in Fig. 1. Without NaOH solution, the products present spherical shape with relatively smooth surface from their TEM and SEM images shown in Fig. 1A and D, respectively. These spheres give an average size of 275 ± 5 nm. Adding 0.5 mL of NaOH aqueous solution into the reaction system leads to the transformation of nickel spheres to chain-like structures with the length of several micrometers and diameter of 250 ± 4 nm (Fig. 1B and E). A rough surface is observed compared to the smooth surface of the spheres. A careful observation reveals that the chains are assembled from spheres via linkage with each other. Continue increasing the volume of NaOH aqueous solution to 2 mL results in the formation of urchin-like structured nickel particles. They behave a spherical skeleton with tips on their surface and their average size is about 150 ± 5 nm (Fig. 1C and F).

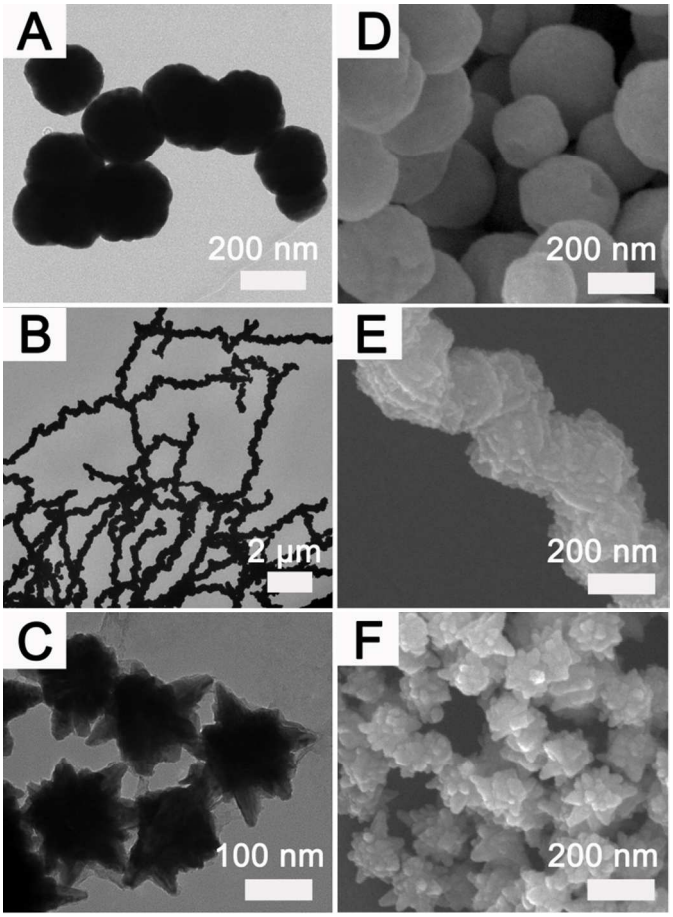

Fig. 1 TEM and SEM images of Ni spheres (A, D), chains (B, E) and urchins (C, F) with addition of 0, 0.5, 2 mL of water and 0, 20, 80 mg of NaOH, respectively.

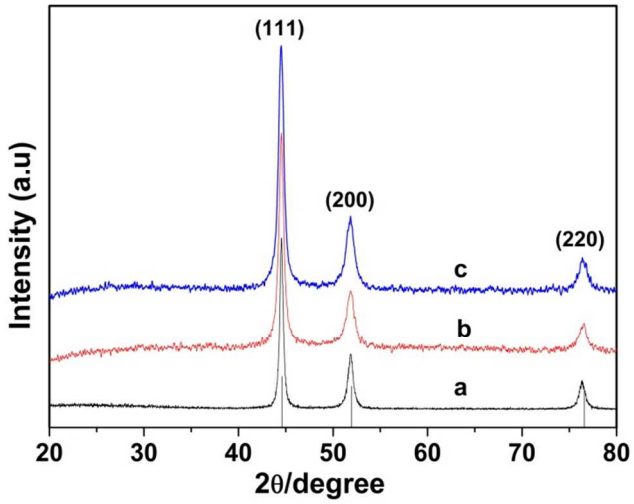

Fig. 2 XRD patterns of Ni spheres (a), chains (b) and urchins (c).

XRD

The XRD patterns of these three samples are shown in Fig. 2. The characteristic diffraction peaks locating at $2\theta = 44.6^{o}$, 51.9^{o} and 76.5^{o} are detected in all products, and these peaks can be assigned to (111), (200), and (220) of the nickel particles (JPDS card no. 70-0989). No other peaks that might be contributed to $Ni(OH)_2$ or other nickel complexes are found, indicating the high purity of these samples.

Magnetic properties

All these samples behave excellent magnetic properties that facilitate their separation from the synthesis systems via an external magnetic field. The magnetic properties of materials are dependent on their morphology and crystallinity.[23] The magnetization curves of different Ni particles at room temperature are shown in Fig. 3. The appearance of a hysteresis loop in all cases confirms their ferromagnetic behavior. Besides, the saturation magnetization (Ms), remnant magnetization (Mr) and coercivity (Hc) values of these Ni particles are recorded in Table 1. It reveals that the chain-like nickel particles present a lower Ms than spherical and urchin-like ones, which may be related to their assembly results induced by a crosslink process (vide infra).

Table 1 Saturation magnetization (Ms), remnant magnetization (Mr) and coercivity (Hc) values for samples

Sample	Ms （emu/g）	Mr（emu/g）	Hc（Oe）
Spheres	50.08	7.18	125.51
chains	42.47	9.51	115.94
Urchins	50.05	7.27	114.29

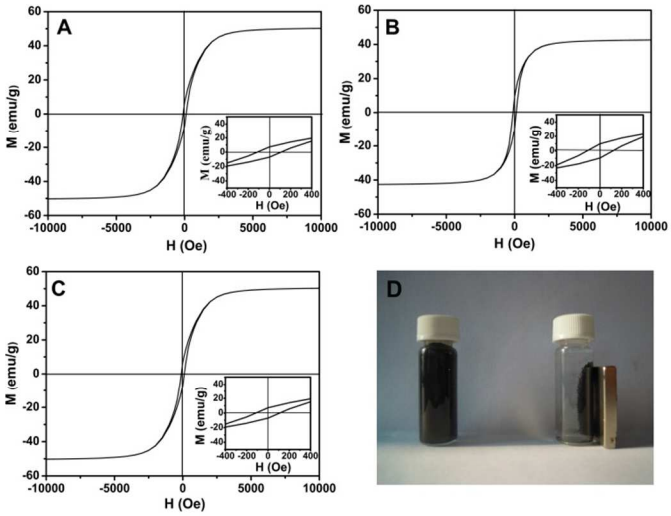

Fig. 3 Magnetic hysteresis loops of Ni spheres (A), chains (B) and urchins (C). (D) The photo for the separation of products with a magnet.

Morphological evolution of nickel particles

In our system, the amount of nickel chloride and the volume of ethylene glycol were kept fixed and the two factors inducing the shape transformation are the volume of water and the amount of NaOH. To make clear the respective roles for water and NaOH, the following experiments were carried out:

1) Solid NaOH salt was added into the synthesis system with the same amount (80 mg) that leads to the generation of urchin-like nanostructured nickel particles while dissolved in 2 mL of water. Under this condition, nickel chains other than urchins were obtained with the diameter of 230 nm and similar rough surface (Fig. 4A).

2) 0.5 and 2 mL of pure water was added into the system instead of NaOH aqueous solution and the resulted products were nickel chains. However, these chains present non-uniform structure with a wide diameter distribution (Fig. 4B and C).

3) In the system containing 0.5 mL of pure water, the addition of 80 mg of NaOH did not result in the formation of nickel urchins. Instead, similar chain-like nickel structures were obtained with the average diameter of 220 nm (Fig. 4D).

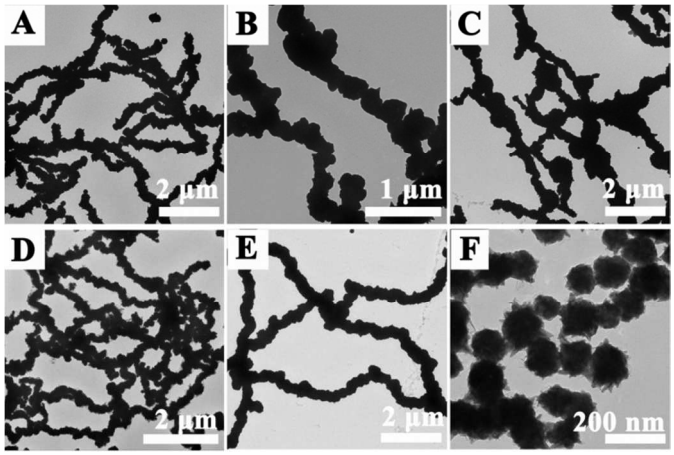

Fig. 4 TEM images of products obtained from different conditions. (A) 80 mg NaOH，(B) 0.5 ml H_2O，(C) 2 ml H_2O，(D) 0.5 ml H_2O + 80 mg NaOH，(E) 20 mg NaOH，(F) 2 ml H_2O + 20 mg NaOH.

Based on the above results, one can find both the water and NaOH play important roles in controlling the formation of different structured nickel particles, especially in achieving urchin-like particles. On one hand, addition of NaOH can greatly improve the reducing ability of the hydrazine hydrate and increase the nucleation rate for the nickel thereby. In the absence of NaOH, fewer nuclei are generated and the following relative fast growth rate leads to the deposition of nickel components owing to the preferred heterogeneous nucleation. This appears much more like a thermodynamic-controlled process and finally spherical shaped nickel particles are achieved in order to minimize the surface energy. In this case, the introduction of just 20 mg of NaOH solid powder can accelerate the nickel nucleation and the polarity of the solvent is also increased, which enhances the magnetic dipole-dipole interaction between the nickel nanoparticles. Therefore, accompanied with the oriented attachment, a fast assembly process is obtained to lead to the formation of the chains (Fig. 4E). It should be noted its surface is a bit smoother than that

from the system with 80 mg of NaOH (Fig. 4A), indicating the strengthened acceleration effect in the later one.

On the other hand, we consider the addition of water also enhances the polarity of the solvents. This change of the polarity similarly tunes the dipole-dipole interaction between the nickel nuclei and a chain-like morphology is achieved. However, under this condition, the surface of the chains appears smoother than that of the products from the system with only NaOH addition (Fig. 4B and C). Besides, a relatively wide distribution of the chain size is observed. This indicates a faster nuclei rate plays certain roles for the uniform assembly of the nanoparticles. It can be confirmed by the resulted uniform nickel chains from a system with addition of 20 or 80 mg of NaOH into the one containing 0.5 mL of water (Fig. 1B and 4D). In the presence of 20 mg of NaOH, increasing the water volume to 2 mL produces particles with rough surface and a few tips (Fig. 4F). This nearly reaches the urchin shape obtained with adding 80 mg of NaOH (Fig. 1C). We consider the increase of the pH in the water/EG mixed solvents other than pure EG system greatly enhances the reducing ability of the hydrazine hydrate, which induces the quicker nucleation process. Once a nucleation centre is formed, the subsequent nickel nuclei rapidly deposits on its surface via the aid of an enhanced dipole-dipole interaction. A fast exhaustion rate of the nickel source materials finally makes the generation of tips on the end of the nickel particles because fewer and fewer nickel particles deposit or grow at the final steps. This could be envisioned as a kinetic controlled process, which guides the formation of urchin-like nanostructures. The decreased particle size compared to spheres or chains also supports the fast nucleation rate (Fig. 1) that forms large amounts of nuclei in the initial step of the reaction.

Therefore, the introduction of water increases the polarity of the solvent to enhance the dipole-dipole interaction between the nickel nanoparticles; while NaOH promotes the nucleation rate along with its similar role to increase the polarity of the solvent. The synergistic effect of the two components guides the transformation of the nickel particles from spherical to chain-like and urchin-like shapes.

In order to further confirm our opinion, the time-dependent experiments for the formation of the different shaped nickel materials were carried out. As for the nickel spheres, no products were collected from the system in 15 min, indicating the slow nucleation rate in the absence of NaOH that could greatly accelerate the reducing ability of the hydrazine hydrate. After 45 min, the spheres were obtained with the size of 220±30 nm (Fig. S1A in ESI†), appearing a wide size distribution. The sphere size turns bigger and the size distribution becomes narrower along with the reaction time (Fig. S1B-C in ESI†) owing to the possible Ostwald ripening. In the initial synthesis process for the nickel chains (15 min), the as-synthesized nickel particles with size of 210±10 nm roughly attached with each other (Fig. S2A in ESI†) because of the dipole-dipole interaction and oriented attachment. Compared with the results for synthesizing nickel spheres, the reaction rate is faster and the size of the particles to assemble chains is smaller, further indicating the effect of the NaOH that facilitates the nucleation kinetics. Along with the reaction time, the chains turns uniform (Fig. S2B-D in ESI†) because the above two possible guidance is strengthened or optimized. As for the nickel urchins, in the first 15 min, sphere-like particles were observed with the size of 60±10 nm (Fig. S3A in ESI†). The particle size is much smaller than that of the nickel spheres and chains due to the accelerated nucleation rate. After the reaction was prolonged to 45 and 90 min, the tips were gradually occurred (Fig. S3B-C in ESI†) because of the further deposition of the rest nickel nuclei. Finally, the urchin-like nickel particles were obtained after 4 h (Fig. S3D in ESI†).

It should be noted, in our system, the ethylene glycol plays as both solvent and reductant. On one hand, the reaction is hardly to generate nickel particles in the absence of ethylene glycol at least in the same period of reaction time (4 h); on the other hand, the ethylene glycol as an organic solvent can prevent the aggregation of the as-synthesized nickel particles.[24]

Catalytic test

As we know, the 4-aminophenol (4-AP) has potential applications in antipyretic drugs, photographic developers and corrosion inhibitors.[25, 26] Therefore, the reduction of 4-NP to 4-AP by $NaBH_4$ in aqueous media was selected as a model reaction to evaluate the catalytic performance of the different morphological nickel particles. Upon addition of $NaBH_4$, the original 4-NP absorption peak at 317 nm shifts to 400 nm due to the formation of 4-nitrophenolateions (Fig. S4 in ESI†).[27, 28] After introduction of the nickel particles, the absorption intensity of the 4-NP at 400 nm decreases and an absorption band at 297 nm is gradually developed, indicating the formation of the 4-AP. The corresponding time-dependent evolution of UV-Vis absorption spectra by using the three shaped nickel particles as catalysts is presented in Fig. 5. The complete degradation of the 4-NP is achieved in 6 min when the urchin-like nickel particles are used; however, it takes 20 and 14 min for spherical and chain-like ones, respectively. Because the concentration of BH_4^- greatly exceeds that of 4-NP, this reaction can be considered as a pseudo-first-order reaction.[29] Therefore, the rate constant (k) is calculated by the slope of the linear fit of ln (C/C_0) versus time, where C/C_0 represents the ratio of 4-NP concentrations at time t and 0. The so-determined k values for spherical, chain-like and urchin-like nickel particles are 0.246, 0.309 and 0.416 min^{-1}, respectively (Fig. 5D). It could be seen the catalytic activity of the urchin-like nickel is 69.1 % and 34.6 % higher than that of the other two.

We consider the highest catalytic performance of the urchin-like nickel particles is related to its unique structure. The presence of the tips endows the particles with much more active points to allow the occurrence of the quick reaction than those in the spheres and chains. This can be further supported by the fact that the chains with a rough surface present a higher catalytic activity than the spheres with a smooth surface. The BET surface area of 8.36, 10.19 and 14.77 $m^2 g^{-1}$ for spherical, chain and urchin-like nickel particles confirms the highest surface activity for the catalytic performance (Fig. 6A).

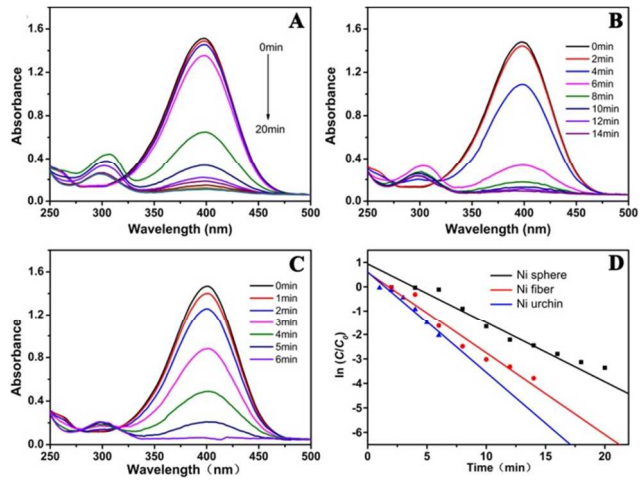

Fig. 5 Time-dependent UV-Vis spectra for the reduction of 4-NP by $NaBH_4$ with nickel spheres (A), chains (B) and urchins (C) as catalysts. (D) The relationship between ln (C/C_0) versus time (t) using different nickel particles.

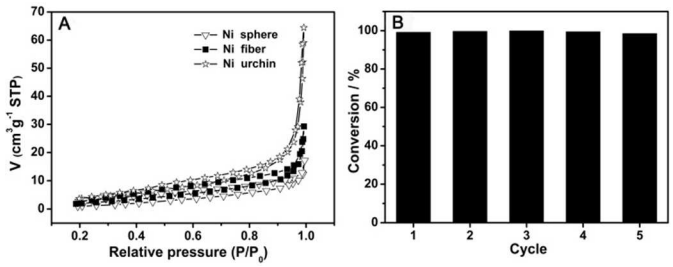

Fig. 6 (A) Nitrogen adsorption-desorption isotherms and (B) the reusability of the urchin-like nickel particles as catalysts for the reduction of 4-NP with $NaBH_4$.

Owing to the excellent magnetic property, the nickel particles can be readily recycled with an external magnetic field (Fig. 3D). The cycle stability of the urchin-like nickel particles was investigated via the aid of a magnet. After 5 rounds, the urchin-like nickel particles still give a high catalytic performance and only 0.67% decrease is detected (Fig. 6B), revealing its high stability without losing the active points during the catalysis process. This can be confirmed by the TEM image of the urchin-like nickel particles after 5 round cycles that nearly no shape transformation or aggregation is observed (Fig. S5 in ESI†).

Conclusions

In summary, we systematically investigated the synthesis of nickel particles in ethylene glycol containing nickel chloride and hydrazine hydrate as nickel source and reductant, respectively. Tuning the amount of water and NaOH in the synthesis system led to the formation of different nickel particles, including spheres, chains and urchins. This was mainly induced by two factors: 1) water changed the polarity of the solvent that strengthened the dipole-dipole interaction between the nickel nuclei; 2) NaOH improved the reducing ability of the hydrazine hydrate that accelerated the reaction rate and a kinetic controlled process was realized. The synergistic effect played an important role in controlling the surface roughness, size and shape, especially in achieving urchin-like nickel particles. Owing to the unique morphology with tips on the particle surface, the urchin-like one presented the highest catalytic performance. Furthermore, the excellent magnetic property made these products readily recycled with almost no activity losing.

Acknowledgements

The authors thank Jilin Provincial Science and Technology Development Foundation (Grant No. 20140101109JC) and National Natural Science Foundation of China (Grant No. 21103018) for financial support.

Notes and references

Faculty of Chemistry, Northeast Normal University, 5268 Renmin Street, Changchun, P.R. China 130024 Tel: (+86) 85099657; E-mail: xingsx737@nenu.edu.cn; liuxc804@nenu.edu.cn

Electronic Supplementary Information (ESI) available: [UV-Vis spectrum and TEM image for corresponding explanation] See DOI: 10.1039/b000000x/

1. C. Deraedt, L. Salmon, S. Gatard, R. Ciganda, R. Hernandez, J. Ruiz and D. Astruc, *Chem. Commun.*, 2014, 50, 14194-14196.
2. M. S. Yavuz, Y. Cheng, J. Chen, C. M. Cobley, Q. Zhang, M. Rycenga, J. Xie, C. Kim, K. H. Song, A. G. Schwartz, L. V. Wang and Y. Xia, *Nat. Mater.*, 2009, 8, 935-939.
3. Y. Tang, Y. Liu, S. Yu, Y. Zhao, S. Mu and F. Gao, *Electrochim. Acta*, 2014, 123, 158-166.
4. X. Ma, J. Liu, C. Liang, X. Gong and R. Che, *J. Mater. Chem. A*, 2014, 2, 12692-12696.
5. M. H. Rashid and T. K. Mandal, *J. Phys. Chem. C*, 2007, 111, 16750-16760.
6. A. R. Tao, S. Habas and P. Yang, *Small*, 2008, 4, 310-325.
7. G. Zhang and L. Zhao, *Dalton. Trans.*, 2013, 42, 3660-3666.
8. X. Ji, X. Song, J. Li, Y. Bai, W. Yang and X. Peng, *J. Am. Chem. Soc.*, 2007, 129, 13939-13948.
9. S. Lv, H. Suo, J. Wang, Y. Wang, C. Zhao and S. Xing, *Colloids Surf., A*, 2012, 396, 292-298.
10. J. E. Millstone, S. J. Hurst, G. S. Métraux, J. I. Cutler and C. A. Mirkin, *Small*, 2009, 5, 646-664.
11. T. T. Chen, F. Deng, J. Zhu, C. F. Chen, G. B. Sun, S. L. Ma and X. J. Yang, *J. Mater. Chem.*, 2012, 22, 15190-15197.
12. Ö. Metin, V. Mazumder, S. Özkar and S. Sun, *J. Am. Chem. Soc.*, 2010, 132, 1468-1469.
13. A. P. LaGrow, B. Ingham, S. Cheong, G. V. Williams, C. Dotzler, M. F. Toney, D. A. Jefferson, E. C. Corbos, P. T. Bishop, J. Cookson and R. D. Tilley, *J. Am. Chem. Soc.*, 2012, 134, 855-858.
14. A. Ghosal, J. Shah, R. K. Kotnala and S. Ahmad, *J. Mater. Chem. A*, 2013, 1, 12868-12878.
15. I. S. Lee, N. Lee, J. Park, B. H. Kim, Y.-W. Yi, T. Kim, T. K. Kim, I. H. Lee, S. R. Paik and T. Hyeon, *J. Am. Chem. Soc.*, 2006, 128, 10658-10659.

16. S. Carenco, C. Boissière, L. Nicole, C. Sanchez, P. Le Floch and N. Mézailles, *Chem. Mater.*, 2010, 22, 1340-1349.
17. D. Liu, X. Wang, D. He, T. D. Dao, T. Nagao, Q. Weng, D. Tang, X. Wang, W. Tian, D. Golberg and Y. Bando, *Small*, 2014, 10, 2564-2569.
18. J. Park, E. Kang, S. U. Son, H. M. Park, M. K. Lee, J. Kim, K. W. Kim, H. J. Noh, J. H. Park, C. J. Bae, J. G. Park and T. Hyeon, *Adv. Mater.*, 2005, 17, 429-434.
19. X. Hu and J. C. Yu, *Chem. Mater.*, 2008, 20, 6743-6749.
20. G. Tontini, A. Koch, V. A. V. Schmachtenberg, C. Binder, A. N. Klein and V. Drago, *Materials Research Bulletin*, 2015, 61, 177-182.
21. S. Senapati, S. K. Srivastava, S. B. Singh and H. N. Mishra, *J. Mater. Chem.*, 2012, 22, 6899-6906.
22. J. Guan, L. Liu, L. Xu, Z. Sun and Y. Zhang, *CrystEngComm*, 2011, 13, 2636-2643.
23. Z. Liu, S. Li, Y. Yang, S. Peng, Z. Hu and Y. Qian, *Adv. Mater.*, 2003, 15, 1946-1948.
24. S.-H. Wu and D.-H. Chen, *J. Colloid Interface Sci.*, 2003, 259, 282-286.
25. J.-S. Shen, Y.-L. Chen, Q.-P. Wang, T. Yu, X.-Y. Huang, Y. Yang and H.-W. Zhang, *J. Mater. Chem. C*, 2013, 1, 2092-2096.
26. Y. Du, H. Chen, R. Chen and N. Xu, *Appl. Catal. A*, 2004, 277, 259-264.
27. A. M. Signori, K. d. O. Santos, R. Eising, B. L. Albuquerque, F. C. Giacomelli and J. B. Domingos, *Langmuir*, 2010, 26, 17772-17779.
28. S. K. Ghosh, M. Mandal, S. Kundu, S. Nath and T. Pal, *Appl. Catal. A*, 2004, 268, 61-66.
29. J. Ge, Q. Zhang, T. Zhang and Y. Yin, *Angew. Chem. In. Ed.*, 2008, 47, 8924-8928.

Graphic Abstract

Nickel shape manipulation from spheres, chains to urchins occurred in ethylene glycol upon addition of different volumes of NaOH aqueous solution. The synergistic effect of water and NaOH played important roles in controlling the morphology of the nickel particles and the urchin-like one presented the highest catalytic performance owing to its unique shape with tips on the surface.